NASA Technical Memorandum 107339
ASME 96–GT–239

Army Research Laboratory
Technical Report ARL–TR–1108

Comparisons of Rig and Engine Dynamic Events in the Compressor of an Axi-Centrifugal Turboshaft Engine

A. Karl Owen
Vehicle Propulsion Directorate
U.S. Army Research Laboratory
Lewis Research Center
Cleveland, Ohio

Duane L. Mattern
NYMA, Inc.
Brook Park, Ohio

Dzu K. Le
Lewis Research Center
Cleveland, Ohio

National Aeronautics and
Space Administration

U.S. ARMY

RESEARCH LABORATORY

COMPARISONS OF RIG AND ENGINE DYNAMIC EVENTS IN THE COMPRESSOR OF AN AXI-CENTRIFUGAL TURBOSHAFT ENGINE

by

A. Karl Owen
U.S. Army Vehicle Propulsion Directorate
NASA Lewis Research Center
Cleveland, Oh, USA

Duane L. Mattern[1]
NYMA, Inc.
NASA Lewis Research Center
Cleveland, Oh, USA

Dzu K. Le
Electronic and Control Systems Division
NASA Lewis Research Center
Cleveland, Oh, USA

1. Now with Scientific Monitoring Inc., Tempe, Az, USA

ABSTRACT

Steady state and dynamic data were acquired in a T55-L-712 compressor rig. In addition, a T55-L-712 engine was instrumented and similar data were acquired. Rig and engine stall/surge data were analyzed using modal techniques. This paper compares rig and engine preliminary results for the ground idle (approximately 60% of design speed) point. The results of these analyses indicate both rig and engine dynamic events are preceded by indications of traveling wave energy in front of the compressor face. For both rig and engine, the traveling wave energy contains broad band energy with some prominent narrow peaks and, while the events are similar in many ways, some noticeable differences exist between the results of the analyses of rig data and engine data.

1.0 INTRODUCTION

Compressors in gas turbine engines are subject to aerodynamic instabilities known as rotating stall and surge if required to operate at or beyond certain massflow/pressure rise/rotor speed points. On the compressor map, these points form a line known as the stall/surge line. When operating in rotating stall or surge, gas turbine engine performance is seriously degraded or impossible. To prevent operation in these regions, the gas turbine cycle is normally designed to allow compressor operation away from the surge line on an "op line". This provides an appropriate margin to insure continued engine operation in the event of unplanned system operation excursions due to, for example, inlet distortion. However, this normally results in accepting less than optimal engine performance. The ability to actively suppress these aerodynamic instabilities would allow operation nearer this surge line, thereby improving gas turbine efficiencies.

Potential improvements in gas turbine engine efficiencies due to active compressor stability enhancement (active stall control) suggest that the development of this technology should be encouraged. Indeed, studies at AlliedSignal (Stratford) indicated a 4.0% reduction in design point specific fuel consumption for the T55 engine (Sehra, 1994) with studies of advanced designs indicating potentially greater improvements. This promised performance improvement has promoted considerable interest in this technology area.

Ludwig et al (1973) demonstrated technology in the 1970s that allowed a turbojet engine to operate with reduced stall margin using active stall control. In the 1980s, Moore and Greitzer (1985) set forth a theory describing the dynamic operation of a compression system as it approached and entered rotating stall/surge. This theory predicted the existence of precursor waves in front of the compression system that would grow into rotating stall. Epstein (1994) first proposed that these precursor waves, if properly analyzed, could be used to guide the operation of an active control system that would extend compression system range. This has been demonstrated on several low speed test compressor rigs independently by Paduano (1992) and by Day (1991), but has yet to be demonstrated in a high speed compressor.

To further the development of this technology, the US Army Vehicle Propulsion Directorate and the NASA Lewis Research Center (LeRC) initiated an effort to demonstrate an "active stability control" device that would increase compression system stability across a broad range of operating speeds in an axi-centrifugal turboshaft engine. The program began with initial rig testing in an AlliedSignal T55-L-712 compressor rig (completed June of 1993). Preliminary analysis of data (Owen, 1994) indicated that precursor waves could be identified in the compression system. A T55-L-712 turboshaft engine was instrumented and installed at LeRC. Testing began March 1995. A proportional high speed valve (Mattern and Owen, 1995) was designed and eight were installed with shroud jet injectors for forced response testing which started June 1995 and ended that October.

This paper compares rig and engine surge events at the ground idle speed. Data presented is from high speed shroud mounted transducers in front of the first stage rotor. Data presented were analyzed using a spatial Fourier analysis technique.
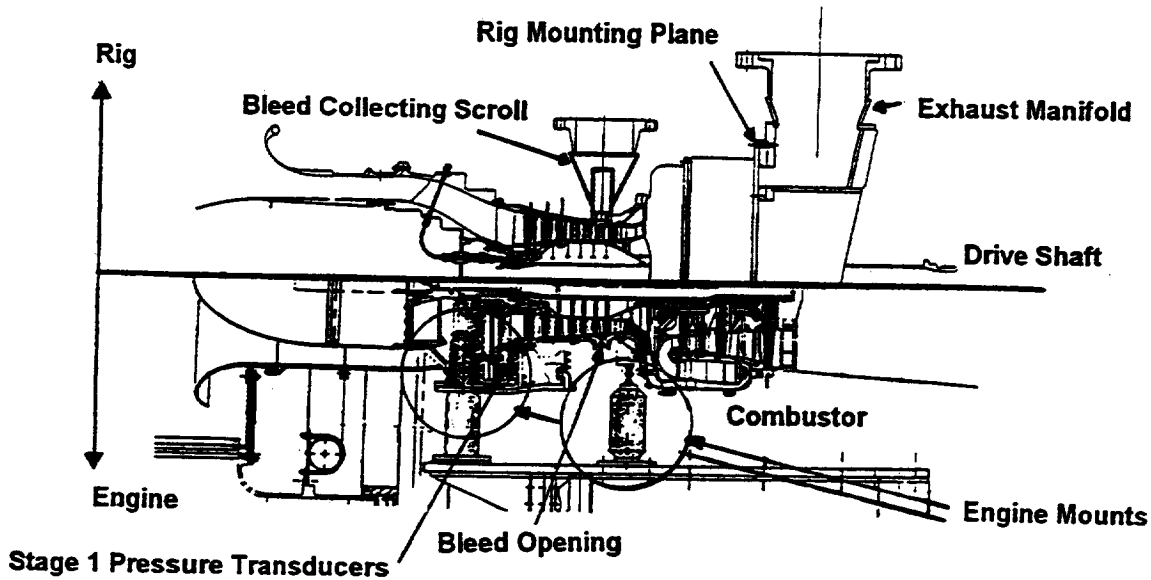
Figure 1. Cutaway Meridional/Radial Views of the Rig and engine Test Facilities

2.0 TEST AND ANALYSIS FACILITIES

2.1 Introduction

References by Owen (1993) and Etter and Hingorani (1993) detail the facility, testing, instrumentation, instrumentation locations, data acquisition, and data reduction methodologies and equipment for the rig testing while Owen (1995) and a NASA Lewis Research Center Pamphlet (1993) provide similar information for the engine testing. Space considerations preclude an extensive review of this information and the interested reader is referred to these references.

Engine testing was divided into two phases, a low speed (ground idle) test and an "all speed" test. The low speed engine testing was conducted with the power turbine locked, since the available dynamometer could not accept the engine power. Engine airflow was measured by integrating massflow at the inlet using total and static pressures and measured temperatures. The compressor operating point was controlled with a start bleed over the sixth stage stator. For "all speed testing", which included additional ground idle testing, a waterbrake system and calibrated bellmouth were acquired, on loan, from AlliedSignal. The waterbrake allowed engine operation over the entire power envelope. The bellmouth improved engine airflow measurements to an accuracy within ± 0.5%. Finally, a combustor inbleed system was designed and installed to allow a more realistic compressor stage matching during the approach to stall/surge.

2.2 Differences Between Engine and Rig

Differences existed between rig and engine test facilities. Figure 1 shows cross sectional views of both the rig and engine. The compressor rig, shown in the upper half of fig. 1, consisted of two sequential research inlet bellmouths, the second attached around an operational engine inlet, a compressor with a standard operational geometry, a downstream plenum nominally sized to simulate a combustor in volume, and an exit throttle valve.

Bleed air was collected in an exit scroll, identified in fig. 1, and exhausted from the building through a duct and controller valve. The rig compressor drive shaft was mounted through the rig to a gearbox and was driven by three T55 engines. In the engine, the downstream plenum was replaced with a combustor and the exit throttle with a turbine. The rig speed was accurately controlled with the three T55 engines while, in the engine, a hydromechanical control unit provided the speed control. Notice in fig. 1 that the compressor rig casing was cantilevered off the plenum housing while the engine was mounted to a test stand at three hard points, two at the 4 and 8 o'clock positions near the first stage of the compressor (two of the operational mounting points) and a single hard point at the 6 o'clock position at the combustor.

2.3 Instrumentation

Differences existed between the rig and engine instrument configurations. Rig instrumentation included a single flush mounted shroud static pressure transducer at every stage starting after stage three and three circumferentially equidistant shroud transducers at the impeller exit. Engine instrumentation included flush mounted hub (wafer) transducers at the exits of the first three stages that confirmed rotating stall began in the tip region. Six Mach probes were located approximately 1 chord length upstream of rotor 1 for the initial portion of the low speed engine testing but were later removed, insuring that these probes would not effect modal wave development.

Significant similarities also existed between rig and engine instrumentation. At each of the first three stages, a set of eight transducers was flush mounted on the shroud at the same axial location. Both rig and engine transducers were at the same circumferential locations and were numbered in order increasing in the direction of rotation. Circumferential increments were approximately 45°. Transducer sizes at a given location, i.e. 15 psi absolute for the stage 1 transducer set, were kept the same between rig and engine and, when possible, the same transducers were used. Figure 1 shows the meridional/radial positions of the flush mounted transducers in front of stage 1.

2

2.4 Data Acquisition and Reduction

For all tests, steady data were acquired consisting of both research and operational parameters sampled at 1 Hz.

For dynamic events on the rig, high bandwidth rig test data (pressure transducers) were recorded on analog tape for later analysis at the LeRC. Low speed dynamic data (up to 80% of design speed) were recorded at 30 IPS (inches per second tape speed), providing a bandwidth of 20 kHz. Rig test data were later digitized at approximately 9000 samples/sec/channel, providing a bandwidth of 3.6 kHz. Engine data were recorded digitally using either the LeRC central data acquisition system or, later, an in-facility data acquisition system. High speed channels were digitized at a rate of about 12750 samples/second/channel, providing a bandwidth of approximately 5 kHz. Critical high speed data were also backed up on tape at a tape speed of at least 30 IPS.

3.0 TEST RESULTS

3.1 Introduction

This section provides comparison of rig and engine dynamic events. A spatial Fourier analysis (SFA) is included in these comparisons. The SFA accomplished on all data used Syed's (1993) implementation of Garnier's (1989) method. Although data from all three stages were analyzed, only the data from the shroud pressure transducers located one chord length upstream of the stage 1 rotor are presented. In this data, as in all high response data acquired during these tests, strong spatial traveling wave energy exists at the rotor frequency. This frequency information was retained for all presented plots, although data were also processed with this signal removed using a notch filter. Data were minimally preprocessed by lowpass filtering at 500 Hz. Both rig and engine data were processed using the same software and filtering techniques. This low pass limit (at over 2.5 rotor frequency) was deemed high enough to allow all pertinent modal information to pass but low enough to eliminate unnecessary noise.

3.2 Rig and Engine Surge Events

To assess differences in surge events caused by the different methods of inducing surge and in test article configurations, the engine was surged with both combustor inbleed and with start bleed closing. The engine was also surged with and without the inlet Mach probes. Figure 2 shows surge event static pressure traces vs time for shroud mounted transducers; one in the rig (fig. 2a) and the others in the engine (one with start bleed and Mach probes (fig. 2b) and one with combustor inbleed and no Mach probes (fig. 2c)). These particular pressure traces were taken from the pressure transducers located at position 1, approximately top dead center on the casing and approximately one chord length upstream of the first stage rotor.

Figure 2a shows two surge pulses (surge frequency ~9 Hz). Superimposed upon these surge pulses, rotating stall cells are discernible. Notice that the distance between rotating stall peaks is greater during the deepest part of the surge event, indicating a change in stall frequency from roughly 65% to 42% of the rotor speed.

Another interesting feature apparent in this plot is in the development of the second surge pulse. Prior to the first surge event (about 8.86 sec), a single rotating stall cell develops but prior to the second surge event (about 8.99 sec) there appear to exist several (probably four) rotating stall cells which merge into a single stronger cell later in the event. This seems to indicate that the boundary conditions the compression
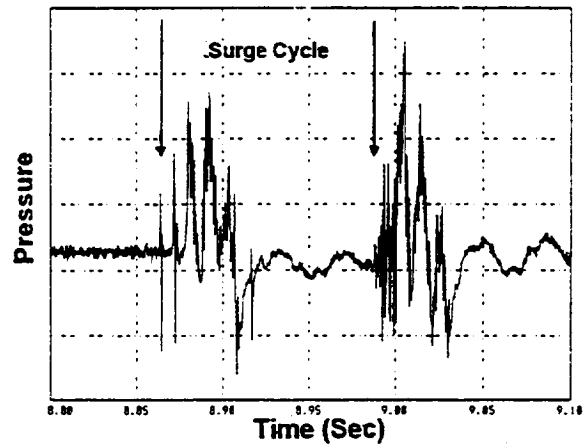
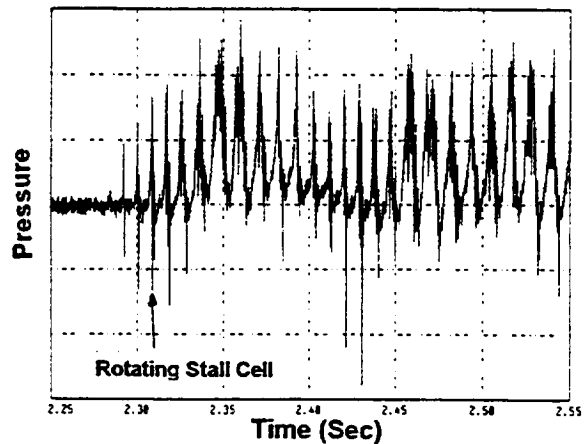

Figure 2a. Compressor Rig Surge

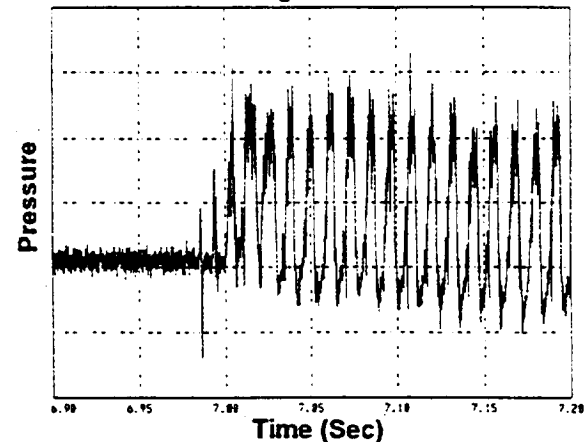**Figure 2b. Engine Surge with Mach Probes Using Start Bleed Band**

Figure 2c. Engine Surge Without Mach Probes Using Combustor Inbleed

Figure 2. Compressor Rig and Full Engine Ground Idle Surges

3

system operates with can effect the number of developing stall cells. During the second event, repressurization to the surge occurred much more rapidly than prior to the first pulse, for example.

Figure 2b is a developing engine dynamic event using start bleed closure and with the inlet Mach probes in position. Apparent are similarities to the rig surge in the shape and frequency of the rotating stall cell. Here, however, the rotating stall appears to develop more slowly, taking twice as many rotations to grow to its largest extent (at 2.37 sec). The presence of the inlet Mach probes did not inhibit the development of this dynamic event. The most striking difference here is the lack of a clear surge pulse. There appears to be a reduction in both steady and peak-to-peak pressure variations or a small partial "clearing" of the event at 2.44 seconds followed by a subsequent deepening of the rotating stall. While it is difficult to accurately measure the length of time between the start of the event and this "clearing", it would appear that it is nearly the same as the time between rig surges (about 0.125 sec).

Figure 2c shows an engine dynamic event similar to the one shown in fig. 2b. However, this event was initiated using combustor inbleed and without the inlet Mach probes. The rotating stall develops more rapidly. This event also shows little indication of surge. Time required for the development of the rotating stalls is the result of the rate at which the test article is driven beyond the stall/surge line. It was difficult to approach and initiate dynamic events in the engine with consistency.

The lack of a clear surge at low speed in the engine is due to the compressor exit boundary conditions. The occurrence of surges, as opposed to rotating stall, are a function of the volume dynamics of the compression system. Since no clear surge pulses occurred, the effective volume in the rig did not match the engine volume. This may, in part, be the result of the engine flameout which occurs immediately after rotating stall begins. The loss of energy input to the air in the combustor may unchoke the turbine, allowing the downstream engine volume to become a part of the system volume. Unfortunately, the low bandwidth of the steady state data acquisition system precluded a direct assessment of this possibility. The use of a rig bleed scroll and throttle valve, since they clearly change the effective system volume, also play a part.

Nonetheless, it is apparent that rotating stalls in this compressor at this speed are similar in both rig and engine, whether induced by start bleed, combustor inbleed, or throttle closure. However, the rate at which rotating stalls are induced can profoundly affect their development.

Lastly, it is interesting to note that the rotating stall event remained present during the entire rig surge event, indicating a very "mild" event with little reverse flow.

3.3 Spatial Fourier Analysis

3.3.1 Introduction

All data shown below were analyzed using a spatial Fourier analysis technique developed by the Massachusetts Institute of Technology and based on the work of Moore and Greitzer. This well known approach postulates the existence of very mild momentum disturbances that travel circumferentially about the front face of the compression system. As the compressor approaches the surge line, the system approaches neutral stability and these disturbances grow. At the rotating stall/surge point, the disturbances initiate or develop into rotating stall/surge. Spatial and temporal variations (in this instance, pressure) sensed in the inlet of the compressor are decomposed into their Fourier components in space about the circumference of the compressor inlet. The number of Fourier components (spatial modes) that can be resolved is a function of the number of sensors. For this application, three rotating modes can be resolved (seven required sensors). Detailed explanations of the technique are presented in Paduano (1992), Garnier (1989), and Tryfonidis (1994).

To develop active stall control devices for turbomachinery applications at least one and possibly three important pieces of information must be extracted by this analysis of the data. First, the approach of rotating stall/surge must be detected with adequate warning time to respond. Second, if two dimensional actuation is desired to inhibit the development of rotating stall/surge, the spatial location in time of those aerodynamic features that promote the development of the dynamic event must be identified. Lastly, the transfer function for the control inputs must be determined. The spatial Fourier analysis is designed, in part, to provide that information. This paper presents an analysis of data to identify the first two pieces of required information.

The figures included in the following sections present analyzed data for approximately the last second prior to the recorded dynamic events. This time interval is a compromise. On one hand, it is a short enough interval to allow a more detailed look at the development of the dynamic events. On the other, the interval is long enough to identify changes that can be used to signal the onset of stall/surge. While this paper cannot present a detailed explanation of the spatial Fourier analysis, a short explanation of the figures is included to help orient the reader.

Figures 3 and 4 show the results of this analysis on rig (figs. 3) and engine (figs. 4) test data. Figure 3a and 4a display the time traces of the eight circumferentially mounted transducers in front of the stage 1 rotor. In these figures, the direction of rotor rotation is up.

Figures 3b and 4b plot the location of the modal wave peak (phase angle) vs non-dimensional time. If a single rate of movement of any of the first three peaks becomes dominant, the rate of change in location becomes constant - the line becomes straight. Note that in fig. 3b, modes 2 and 3 are virtually overlaid and difficult to distinguish. Figures 3c and 4c show the magnitudes of the modal waves.

Figures 3d,e,f and 4d,e,f present the power spectral densities (PSD) for the first, second, and third modes for their respective data sets. These plots present the overall power as a function of frequency for the acquired datasets. These are plotted with frequency on the abscissa and a non-dimensional magnitude on the ordinate. In these plots the "traveling wave" is indicated by the difference between the two plotted lines at a given frequencies. If the plotted solid line has a greater magnitude at a given frequency than the dotted line, the wave is moving in the direction of rotation. If both the solid line and the dashed line are the same magnitude, the wave is spatially stationary. Large differences between the two lines, such as those shown in fig. 3d at 1 rotor frequency (RS) indicate a strong modal energy at that frequency. These plots indicate at what frequencies the largest traveling wave energies exist. To assess if certain frequency ranges become more prominent as the machine approaches stall/surge, this calculation is done using a "traveling window" and shown in figs. 3h,i,j and 4h,i,j. These magnitudes are calculated for a window fifty samples wide. They are calculated and displayed every ten sample steps during the approach to stall/surge.

Figures 3g and 4g show a non-dimensional integrated total traveling wave energy vs time from Tryfonidis (1994). This represents the total modal or traveling energy for all frequencies contained in the data.

All of these types of information have been used previously to identify the approach to rotating stall/surge in various compression systems.

3.3.2 Rig Test Results

Figures 3 show the results of an SFA on data acquired during a rig surge. The roughly linear phase shifts for mode 1 and, to a lesser extent, modes 2 and 3, in fig. 3b indicate strong phase tracking over the entire presented time interval up to the defined surge event at approximately 182 rotor revolutions (RR). However, the slight variations in phase change indicate that no single modal frequency dominates (notice the large vertical axis scale). The possible existence of standing waves will also tend to destroy phase angle tracking of a single frequency. Certain segments show tracking at near the rotor frequency (RS), for example near 50 and again at 100 rotor revolutions. Although difficult to see, between 155 and 180 rotor revolutions, the mode 3 phase angle plot shows phase angle tracking near 60% of RS. When the rotor frequency is filtered out, certain segments of the mode 1 track also show clear tracking at ~60% of the rotor speed. Figure 3c shows that no increase in SFC magnitudes occurs during this interval.

The PSD spectral magnitudes (figs. 3d,e,f) plots indicate the reason for this behavior.. Modes 1 and 3 contain broad bands of positive traveling wave energy with peaks at 1 RS and 2 RS. The mode 2 plot shows no traveling wave content other than a negative traveling wave at 2 RS. Over most of the frequency ranges analyzed, the positive (solid line) PSD is larger than the negative PSD. The phase angle plots reflect this since the modal waves do not show a single dominant frequency but do show positive (in the direction of rotor rotation) traveling wave tracking.

In fig. 3g, the mode 1 moving window PSD, two "ridges" shown are at 60% and 100% of the rotor frequency. Apparent at approximately 150 rotor revolutions is a growth in the PSD magnitude at 60% of the rotor speed and a reduction of the 100% PSD magnitude. This peak then drops off and the surge begins. The mode 2 PSD (fig. 3i) plot shows increased PSD magnitudes at -1.25 times the rotor speed but no clear change in the magnitude prior to surge. The mode 3 plot (fig. 3j) indicates growth prior to stall with damping immediately prior to stall.

Tryfonidis et al. (1994) suggested an increase in traveling wave energy may be a robust indicator of impending stall/surge but noted that 70% speed data from the T55 compressor rig did not show a prominent traveling wave energy increase. This appears true at ground idle (fig. 3f).

In summary, a spatial Fourier analysis of rig test data acquired in front of the first stage rotor indicates the existence of traveling waves. Changes in PSD magnitudes may indicate an impending stall event. However, no single wave frequency dominates the approach to stall.

3.3.3 Engine Test Results

Figures 4 show the results of a spatial Fourier analysis of a ground idle surge induced using combustor inbleed without inlet Mach probes.

Phase angle tracking is apparent (fig. 4b). But no mode clearly shows constant rate of phase change approaching stall to indicate a single dominant frequency. However, the mode 1 results do show considerable intervals of tracking at ~132% RF (for example at ~80 RR). This tracking is broken up intermittently. Also, the mode 2 signals show periods of tracking at near the stall cell frequency (~60% RS). All modes clearly track the rotating stall cell from 190 RR. The SFC magnitudes (fig. 4c), like the rig results, show little indication of impending stall.

The overall PSD plots shown in figs. 4d,e,f show strong traveling energy at a number of discrete frequencies. Specifically, substantial energy exists at 0.9, 1.0, 1.32, 1.8, and 2.0 RS. Mode 1 indicates traveling at 0.9, 1.0, and 1.8. Also, this mode shows a broad traveling energy band up to ~1.2 RS. The strongest energy resides at 1.32 RS and this is

reflected in the phase angle plot. Mode 2 shows only strong traveling wave energy at 1.8 RS, although some exists at 0.9 and 1.32. This 1.8 RS energy would suggest modal phase tracking at 0.9 RS and, although this frequency tracking is apparent at some times in the signal (~180 RR), it does not dominate the phase angle tracking. Broad traveling wave energy is shown in the mode 1 and 3 plots, although it is more prominent in the mode 3 results. The strongest traveling wave frequencies in the mode 3 data are at 1.8 and 2.0 RS. Implying traveling wave frequencies at 0.6 and 0.66 RS (both near the rotating stall frequency).

The calculations of PSD magnitudes using the sliding windows show no noticeable transfer of energy between frequencies or growth of the PSD at any given frequency. As with the rig test data, the traveling wave energy shows little change during the approach to surge (fig. 4g). The PSD plotted vs time (figs. 4,h,i,j) show only minor changes with no clear indicator of impending surge.

3.3.4 A Comparison of Rig and Engine Surges

In general, an analysis of both rig and engine data show strong indications of spatially traveling waves for all three modes. However, no single frequency appears to dominate any analyzed spatial mode. Also common to both rig and engine test data is significant RS signal content.

It is also apparent that calculations of SFC magnitude, PSD magnitudes (traveling window), and total traveling wave energy do not provide any clear predictor of rotating stall/surge onset for either configuration.

While significant similarities exist between the rig and engine dynamic events, notable differences also exist. The phase angle tracking during the engine dynamic event shows distinct periods of tracking at a single modal frequency (mode 1 at 1 RS, and mode 2 at ~0.60 RS). The rig data also shows some mode 2 and 3 tracking at ~0.60 RS.

Engine PSD plots show a far richer content of single frequency peaks than equivalent rig data. Table 1 presents frequencies where PSD magnitudes peak for rig (tagged with an R) and engine (tagged with an E) events. Peaks not indicating spatial movement are tagged with an S.

Table 1:

PSD Frequency Peaks		
Mode 1	Mode 2	Mode 3
0.9 E	0.9 E	0.9 E
1.0 E, 1.0 R	1. 0 ES,1.0 RS	
1.32 E	1.32 E	1.32 E
1.8 ES	1.8 E	1.8 E
2.0 E, 2.0 R	2.0 ES, 2.0 R	2.0 E, 2.0 R

4.0 CONCLUSIONS

The following conclusions can be made:

1) Rig and engine test data taken by eight flush mounted shroud pressure transducers located about the compressor inlet one chord length in front of the first stage rotor contain strong modal information. However, no single frequency dominates any mode during the approach to rotating stall/surge. This supports the modal description of rotating
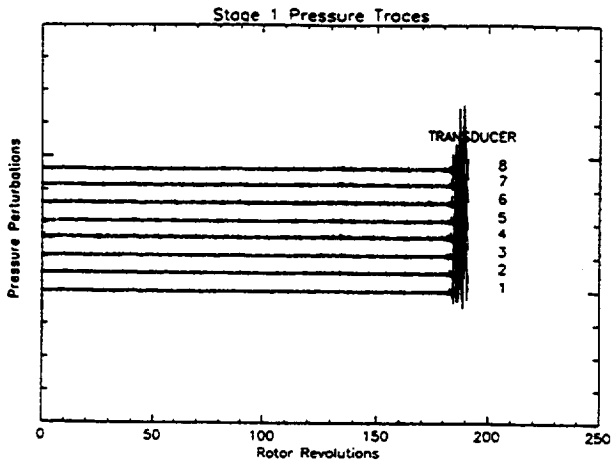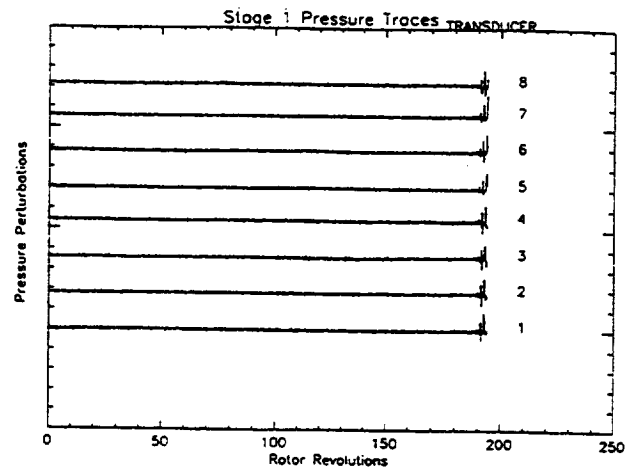
Figure 3a. Transducer Pressure Traces vs Time

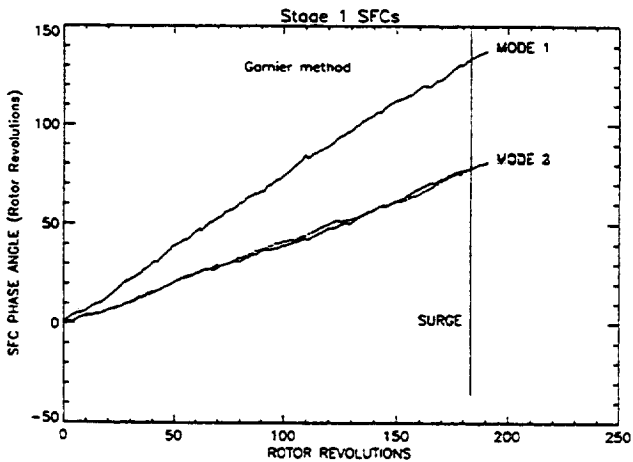**Figure 4a. Transducer Pressure Traces vs Time**

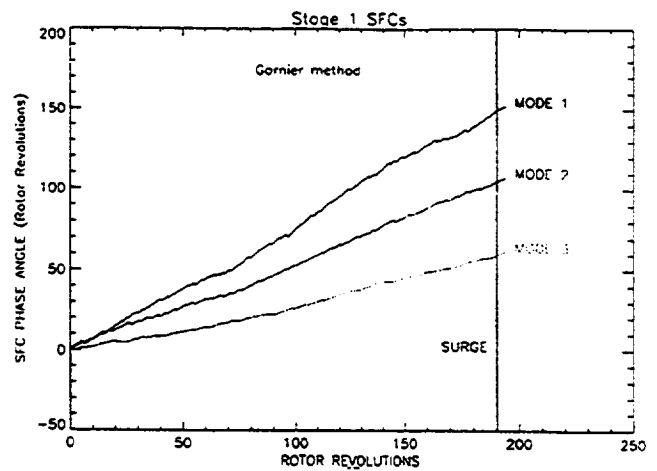**Figure 3b. SFC Phase Angles vs Time**
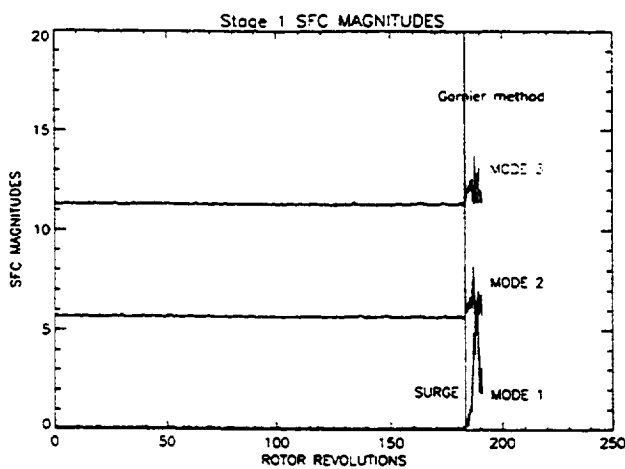

Figure 4b. SFC Phase Angles vs Time

Figure 3c. SFC Magnitudes vs Time

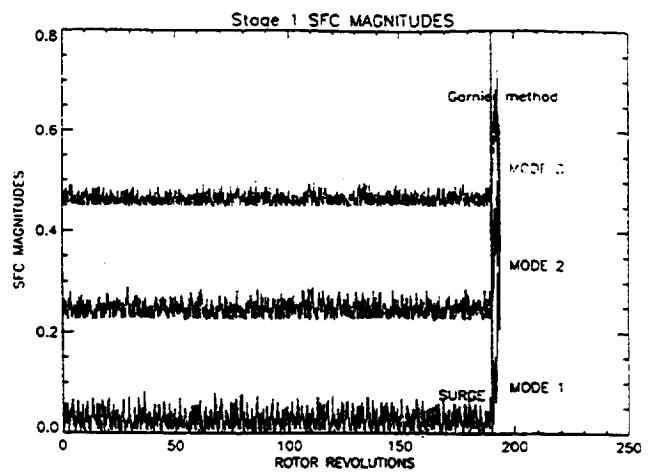**Figure 3. Spatial Fourier Analysis,
Rig Dynamic Event**

Figure 4c. SFC Magnitudes vs Time

**Figure 4. Spatial Fourier Analysis,
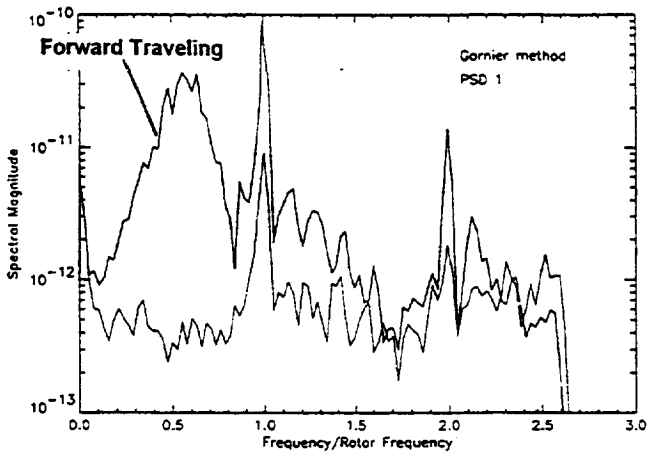Engine Dynamic Event**
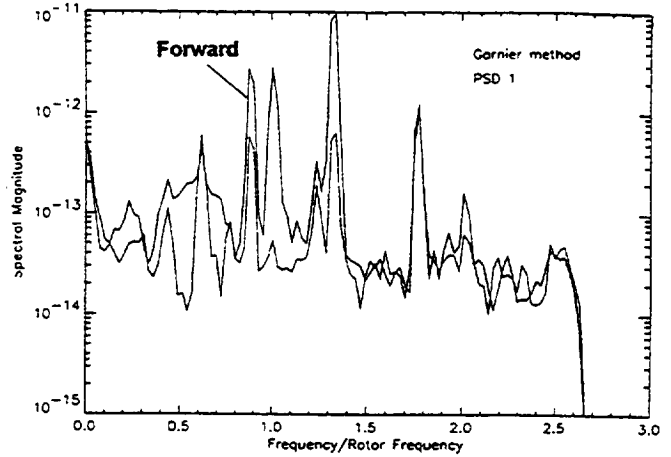
6

Figure 3d. Mode 1 Power Spectral Density vs Frequency

Figure 4d. Mode 1 Power Spectral Density vs Frequency
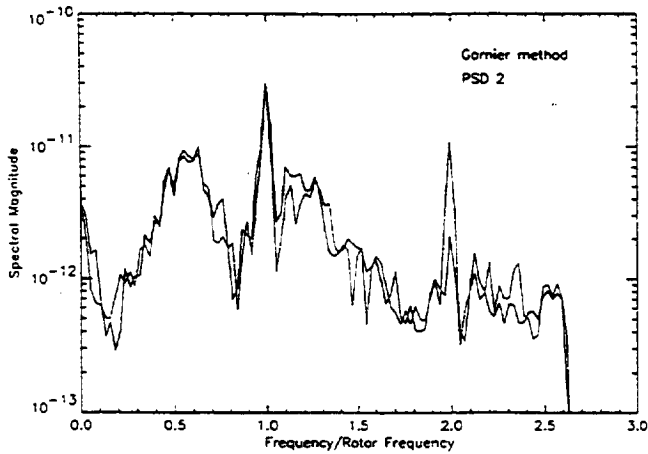
Figure 3e. Mode 2 Power Spectral Density vs Frequency
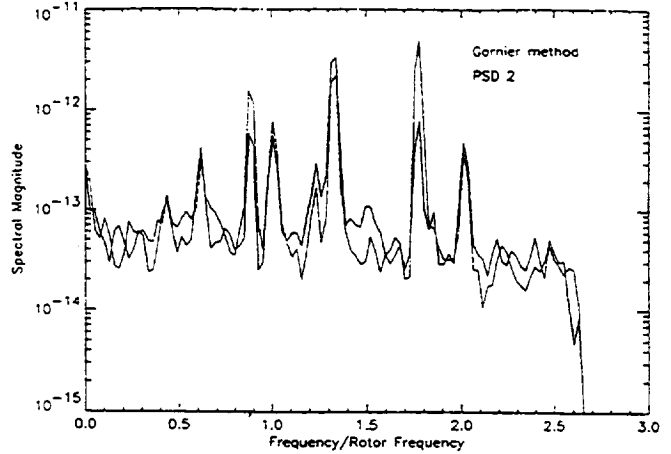
Figure 4e. Mode 2 Power Spectral Density vs Frequency
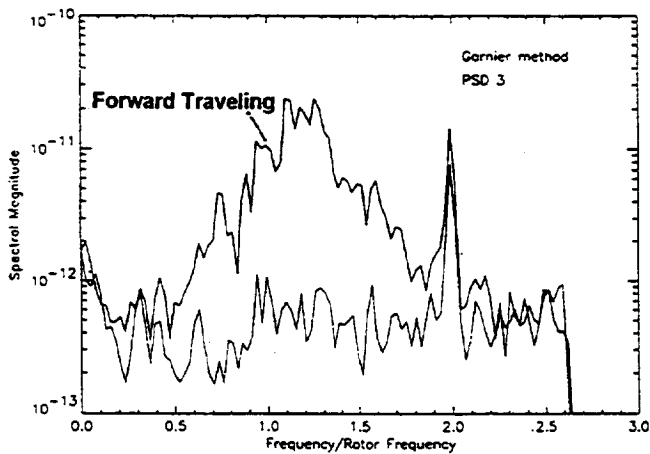
Figure 3f. Mode 3 Power Spectral Density vs Frequency

**Figure 3. Spatial Fourier Analysis,
Rig Dynamic Event, Continued**
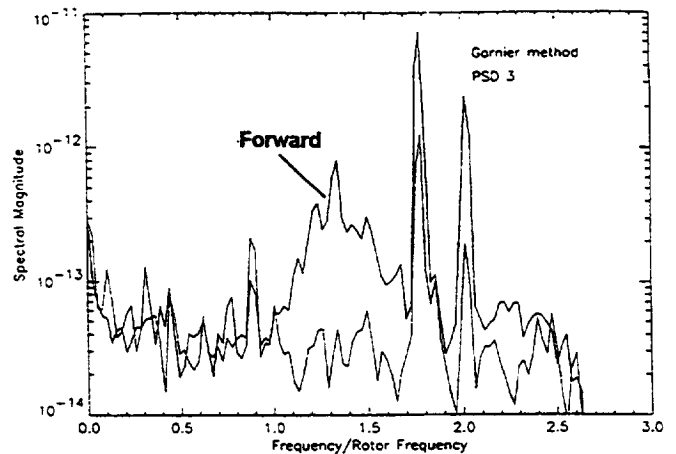
Figure 4f. Mode 3 Power Spectral Density vs Frequency

**Figure 4. Spatial Fourier Analysis,
Engine Dynamic Event, Continued**

7

Figure 3g. Traveling Wave Energy vs Time
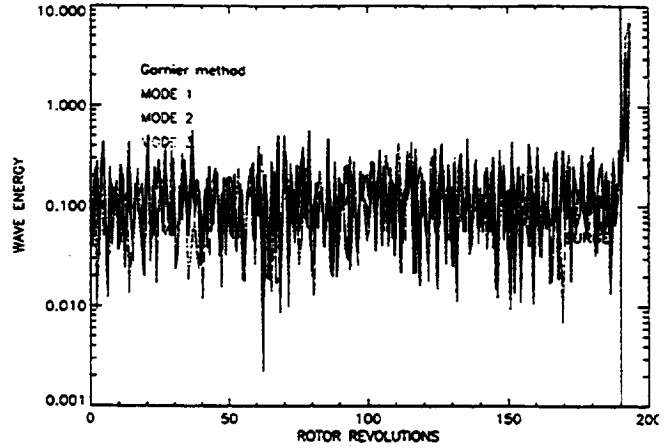
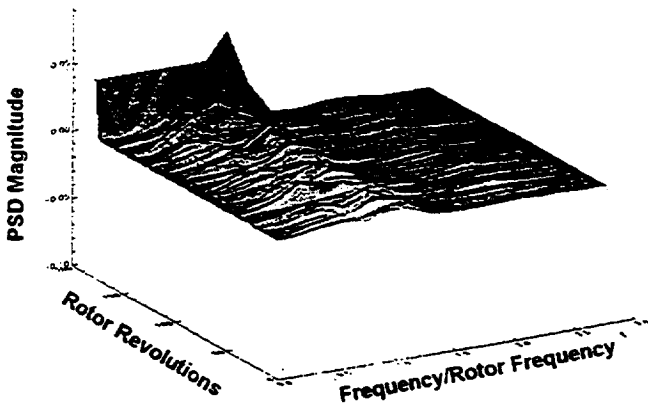**Figure 4g. Traveling Wave Energy vs Time**

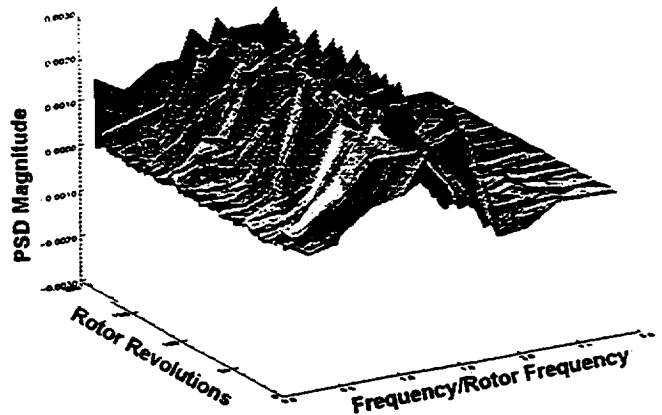**Figure 3h. Mode 1 PSD vs Frequency vs Time**

Figure 4h. Mode 1 PSD vs Frequency vs Time
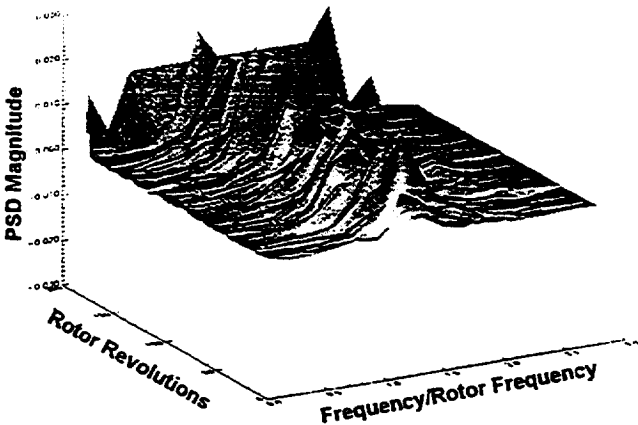

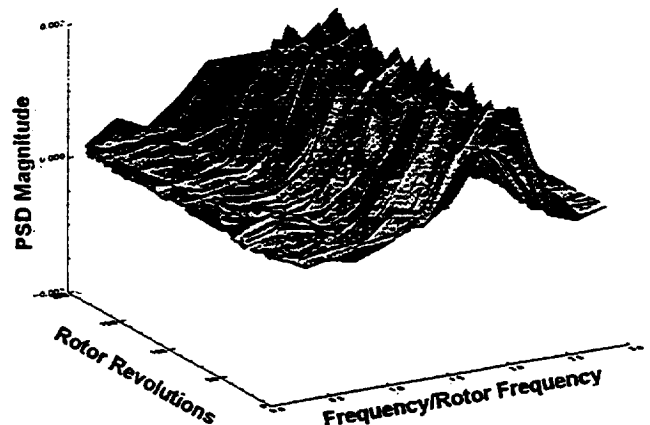**Figure 3i. Mode 2 PSD vs Frequency vs Time**

Figure 4i. Mode 2 PSD vs Frequency vs Time

**Figure 3. Spatial Fourier Analysis,
Rig Dynamic Event, Continued**

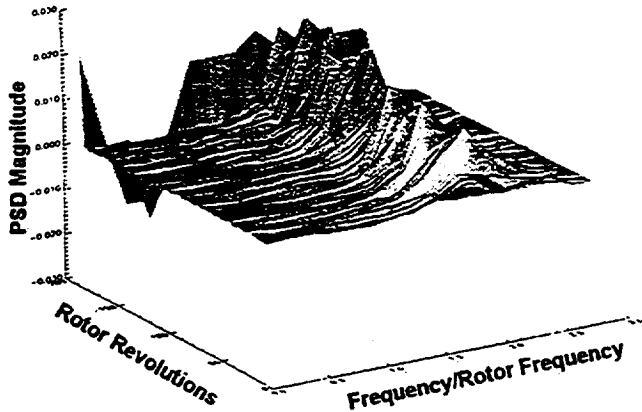**Figure 4. Spatial Fourier Analysis,
Engine Dynamic Event, Continued**

8

Figure 3j. Mode 3 PSD vs Frequency vs Time

Figure 3. Spatial Fourier Analysis,
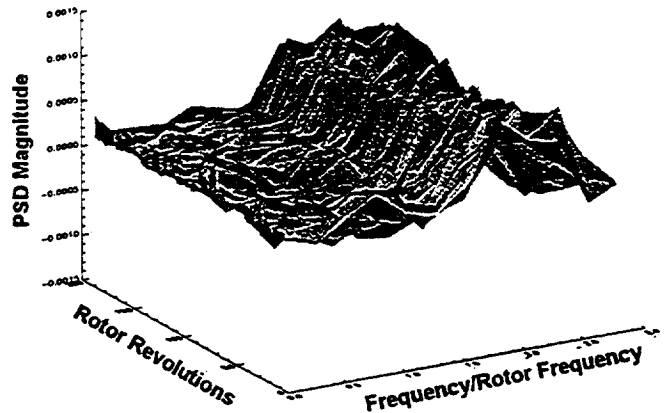Rig Dynamic Event, Continued

Figure 4j. Mode 3 PSD vs Frequency vs Time

Figure 4. Spatial Fourier Analysis,
Engine Dynamic Event, Continued

stall/surge development.

2) The modal analysis of both rig and engine data does not provide a robust indication of the onset of rotating stall/surge. However, considerably more work must be done to improve the results of this analysis.

3) Significant differences between the results of modal analyses of rig and engine data suggest that the development of an active stability enhancement device requires an analysis of both rig and engine data.

4) The rate at which the compressor is forced into rotating stall/surge may significantly effect the development of the event. This could explain some of the differences between the modal analysis results of the rig and engine dynamic events. In addition, the relatively rapid repressurization prior to the second rig surge pulse apparently led to multiple rotating stall cells that were not apparent in the first surge pulse.

5) Both rig and engine rotating stall events are similar in shape and frequency. However, the engine lacks a distinct surge pulse at 60% of design speed. It is not clear whether this is the result of the differences in geometry or test techniques.

REFERENCES

Day, I.J.,"Active Suppression of Rotating Stall and Surge in Axial Compressor", ASME Paper 91-GT-87, June 1991.

Epstein, A.H., Ffowcs Williams, F.E., and Greitzer, E.M., "Active Suppression of Compressor Instabilities", AIAA 10th Aeroacoustic Conference, AIAA, July, 1986, AIAA-86-1994.

Etter, S. and Hingorani, S., "T55-L-712 Start-Up Stall Investigation, Contract NAS3-26698, TEST PLAN", May 5, 1993,(Proprietary).

Garnier, V.H., "Experimental Investigation of Rotating Waves as a Rotating Stall Inception Indication in Compressors", Gas Turbine Laboratory Report GTL #198, Massachusetts Institute of Technology, Nov 1989.

Ludwig, G.R., Nenni, J.P. and Arendt, R.H., "Investigation of Rotating Stall in Axial Flow Compressors and the Development of a Prototype Rotating Stall Control System", Technical Report AFAPL-TR-73-45, May, 1973.

Mattern, D.L., and Owen A.K. "A Voice Coil Actuated Air Valve for Use in Compressor Forced Response Testing", presented at the 1995 SPIE Aerosense Conference, Orlando, Fl, SPIE Vol 2494, paper #2494-19.

Moore, F.K., and Greitzer, E.M.,"A Theory of Post-Stall Transients in Axial Compression Systems: Parts I-II", ASME Paper No. 85-GT-172, 1985.

Owen, A.K., "Analysis of Rig Test Data for an Axial/Centrifugal Compressor in the 12 Kg/Sec Class", Presented at the AGARD 82nd PEP, Montreal, Can., Oct 4-8, 1993.

Owen, A.K. and Bobula, G.A., "Analysis of Dynamic Rig Test Data for an Axial/Centrifugal Compressor Operating at Design Speed", Presented at the AHS 50th Annual Forum and Technology Display, May 11-13, 1994.

Owen, A.K., "An Analysis of Unsteady Aerodynamic Events in a Gas Turbine Generator Compressor", presented at the 19th Army Science Conference, Orlando, Fl, June 20-23, 1994.

Owen, A.K.,"Comparisons Between Unsteady Aerodynamic Events in a Gas Turbine Generator and an Identical Compressor Rig", Presented at the AGARD 85th PEP, Derby, GB, May 8-12,1995.

Paduano, J.D., "Active Control of Rotating Stall in Axial Compressors", PhD Dissertation, Massachusetts Institute of Technology, GTL Report #208, March, 1992

Sehra, A.K., "The Promise of Active control for Helicopter and Tank Engines", Workshop on Intelligent Turbine Engines for Army Applications, Cambridge, Ma, March 21-22,1994.

Syed, O.A. Personal communication, March 1994.

"The Engine Components Research Laboratory", Aeropropulsion Facilities and Experiments Division, Lewis Research Center, Aug 1993.

Tryfonidis, M., Etchevers, O., Paduano, J.D., Epstein, A.H. and Hendricks G.J.,"Pre-Stall Behavior of Several High-Speed Compressors", Presented at the ASME IGTI, the Hague, Netherlands, Jun 1994.

REPORT DOCUMENTATION PAGE

Public reporting burden for this collection of information is estimated to average 1 hour per response, including the time for reviewing instructions, searching existing data sources, gathering and maintaining the data needed, and completing and reviewing the collection of information. Send comments regarding this burden estimate or any other aspect of this collection of information, including suggestions for reducing this burden, to Washington Headquarters Services, Directorate for Information Operations and Reports, 1215 Jefferson Davis Highway, Suite 1204, Arlington, VA 22202-4302, and to the Office of Management and Budget, Paperwork Reduction Project (0704-0188), Washington, DC 20503.

1. AGENCY USE ONLY (Leave blank)	2. REPORT DATE October 1996	3. REPORT TYPE AND DATES COVERED Technical Memorandum

4. TITLE AND SUBTITLE

Comparisons of Rig and Engine Dynamic Events in the Compressor of an Axi-Centrifugal Turboshaft Engine

5. FUNDING NUMBERS

WU-505-62-0L

6. AUTHOR(S)

A. Karl Owen, Duane L. Mattern, and Dzu K. Le

7. PERFORMING ORGANIZATION NAME(S) AND ADDRESS(ES)

NASA Lewis Research Center
Cleveland, Ohio 44135-3191
and
Vehicle Propulsion Directorate
U.S. Army Research Laboratory
Cleveland, Ohio 44135-3191

8. PERFORMING ORGANIZATION REPORT NUMBER

E-10478

9. SPONSORING/MONITORING AGENCY NAME(S) AND ADDRESS(ES)

National Aeronautics and Space Administration
Washington, D.C. 20546-0001
and
U.S. Army Research Laboratory
Adelphi, Maryland 20783-1145

10. SPONSORING/MONITORING AGENCY REPORT NUMBER

NASA TM-107339
ARL-TR-1108
ASME 96-GT-239

11. SUPPLEMENTARY NOTES

Prepared for the 41st Gas Turbine and Aeroengine Congress sponsored by the International Gas Turbine Institute of the American Society of Mechanical Engineers, Birmingham, United Kingdom, June 10-13, 1996. A. Karl Owen, Vehicle Propulsion Directorate, U.S. Army Research Laboratory, NASA Lewis Research Center; Duane L. Mattern, NYMA, Inc., 2001 Aerospace Parkway, Brook Park, Ohio 44142 (work funded by NASA Contract NAS3-27186) now with Scientific Monitoring, Inc., Tempe, Arizona; Dzu K. Le, NASA Lewis Research Center. Responsible person, A. Karl Owen, organization code 2760, (216) 433-5895.

12a. DISTRIBUTION/AVAILABILITY STATEMENT

Unclassified - Unlimited
Subject Category 07

This publication is available from the NASA Center for AeroSpace Information, (301) 621-0390.

12b. DISTRIBUTION CODE

13. ABSTRACT (Maximum 200 words)

Steady state and dynamic data were acquired in a T55-L-712 compressor rig. In addition, a T55-L-12 engine was instrumented and similar data were acquired. Rig and engine stall/surge data were analyzed using modal techniques. This paper compares rig and engine preliminary results for the ground idle (approximately 60% of design speed) point. The results of these analyses indicate both rig and engine dynamic event are preceded by indications of traveling wave energy in front of the compressor face. For both rig and engine, the traveling wave energy contains broad band energy with some prominent narrow peaks and, while the events are similar in many ways, some noticeable differences exist between the results of the analyses of rig data and engine data.

14. SUBJECT TERMS

Stall; Surge; Spatial fourier analysis; Wavelet analysis

15. NUMBER OF PAGES
11

16. PRICE CODE
A03

17. SECURITY CLASSIFICATION OF REPORT	18. SECURITY CLASSIFICATION OF THIS PAGE	19. SECURITY CLASSIFICATION OF ABSTRACT	20. LIMITATION OF ABSTRACT
Unclassified	Unclassified	Unclassified	